Geochemistry Geophysics Geosystems G3

Article
Volume 14, Number 1
30 January 2013
doi:10.1029/2012GC004330
ISSN: 1525-2027

Published by AGU and the Geochemical Society

Incorporation of uranium in benthic foraminiferal calcite reflects seawater carbonate ion concentration

Nina Keul
Alfred Wegener Institute, Bremerhaven, Germany (nkeul@ldeo.columbia.edu)

Now at: Lamont-Doherty Earth Observatory, Columbia University, Palisades, New York, USA

Gerald Langer
Department of Earth Sciences, Cambridge University, Cambridge, UK

Lennart Jan de Nooijer
Department of Marine Geology, Royal Netherlands Institute of Sea Research, Horntje, The Netherlands

Gernot Nehrke
Alfred Wegener Institute, Bremerhaven, Germany

Gert-Jan Reichart
Department of Marine Geology, Royal Netherlands Institute of Sea Research, Horntje, The Netherlands

Alfred Wegener Institute, Bremerhaven, Germany

Jelle Bijma
Alfred Wegener Institute, Bremerhaven, Germany

Earth and Space Sciences, Jacobs University, Bremen, Germany

[1] The chemical and isotopic composition of foraminiferal shells (so-called proxies) reflects the physicochemical properties of the seawater. In current day paleoclimate research, the reconstruction of past seawater carbonate system to infer atmospheric CO_2 concentrations is one of the most pressing challenges, and a variety of proxies have been investigated, such as foraminiferal U/Ca. Since in natural seawater and traditional CO_2 perturbation experiments the carbonate system parameters covary, it is not possible to determine the parameter of the carbonate system causing, e.g., changes in U/Ca, complicating the use of the latter as a carbonate system proxy. We overcome this problem by culturing the benthic foraminifer *Ammonia* sp. at a range of carbonate chemistry manipulation treatments. Shell U/Ca values were determined to test sensitivity of U incorporation to various parameters of the carbonate system. We argue that $\left[CO_3^{2-}\right]$ is the parameter affecting the U/Ca ratio and consequently, the partitioning coefficient for U in *Ammonia* sp., D_U. We can confirm the strong potential of foraminiferal U/Ca as a $\left[CO_3^{2-}\right]$ proxy.

Components: 6,400 words, 3 figures, 2 tables.

Keywords: U/Ca; benthic foraminifera; Ammonia; carbonate chemistry; Uranium partitioning coefficient.

©2013. American Geophysical Union. All Rights Reserved.

Index Terms: 0419 Biogeosciences: Biomineralization; 0473 Biogeosciences: Paleoclimatology and paleoceanography (3344, 4900).

Received 3 July 2012; **Revised** 5 November 2012; **Accepted** 30 November 2012; **Published** 30 January 2013.

Keul, N., G. Langer, L. J. de Nooijer, G. Nehrke, G.-J. Reichart, and J. Bijma (2013), Incorporation of uranium in benthic foraminiferal calcite reflects seawater carbonate ion concentration, *Geochem. Geophys. Geosyst.*, *14*, 102–111, doi:10.1029/2012GC004330.

1. Introduction

[2] Reconstruction of past atmospheric CO_2 concentrations is one of the most pressing challenges in current day paleoclimate research. Climate sensitivity due to atmospheric CO_2 doubling will likely cause global temperature to increase by 2.0–4.5°C [*International Panel on Climate Change* (*IPCC*), 2007]. While the direct effect of increasing CO_2 is straightforward, the eventual impact of CO_2 rise is uncertain due to the various positive and negative feedbacks in the climate system. In combination with temperature reconstructions, accurate atmospheric paleo-CO_2 estimates are necessary to validate models that aim at predicting global temperature rise related to CO_2-forcing mechanisms. Reconstructions of atmospheric pCO_2 from ice cores are confined to the last 800 kyr [*Lüthi et al.*, 2008], while reconstruction of atmospheric pCO_2 going further back in time relies on sedimentary archives [e.g., *Hönisch et al.*, 2012]. Within the latter, foraminifera play a central role since the chemical and isotopic composition of their shells reflects the physicochemical properties of the seawater that these organisms grew in [*Emiliani*, 1955].

[3] On glacial-to-interglacial timescales, atmospheric CO_2 concentrations are largely driven by the amount of dissolved inorganic carbon in the ocean since the latter functions as a large reservoir of CO_2 being in equilibrium with the atmosphere [*Broecker and Peng*, 1982]. Consequently, past seawater [CO_2(aq)] may be used to estimate paleo-atmospheric CO_2. To reconstruct paleo-seawater [CO_2(aq)], two out of six parameters of the ocean's carbonate system ([CO_2], $\left[HCO_3^-\right]$, $\left[CO_3^{2-}\right]$, pH, DIC (total dissolved inorganic carbon), and TA (total alkalinity)) must be known.

[4] Foraminiferal boron isotopes are known to reflect seawater pH [*Hemming and Hanson*, 1992; *Hönisch et al.*, 2009; *Sanyal et al.*, 1995] and hence are used to reconstruct paleo-seawater pH [*Hönisch et al.*, 2009]. A second carbonate system parameter needed to complete past atmospheric CO_2 concentration calculations could be total alkalinity, which can be estimated from reconstructed changes in salinity [*Hönisch and Hemming*, 2005]. The uncertainty that is associated with such salinity reconstructions (derived from combining foraminiferal $\delta^{18}O$ measurements with an independent temperature proxy such as Mg/Ca) [*Nürnberg et al.*, 1996], however, call for a direct, independent proxy for one of the other carbonate system parameters. Foraminiferal B/Ca is thought to reflect $\left[CO_3^{2-}\right]$, but the errors in reconstructed carbonate ion concentrations may be too large to reliably reconstruct the complete carbonate system and thus paleo-pCO_2 [*Yu and Elderfield*, 2007; *Yu et al.*, 2010].

[5] The U/Ca ratio of both planktic and benthic foraminifera is known to correlate with carbonate system parameters such as pH and $\left[CO_3^{2-}\right]$ [*Raitzsch et al.*, 2011; *Russell et al.*, 2004] and hence is a potential alternative to the B/Ca ratio to reconstruct seawater $\left[CO_3^{2-}\right]$. It is, however, not known which of these correlations represent a causal relationship and which correlations are merely accidental regularities. To make this distinction, experiments are necessary in which different parameters of the carbonate system are manipulated independently. The classical approach in carbonate chemistry perturbation experiments [*Smith and Roth*, 1979] is insufficient since this changes several parameters of the carbonate system simultaneously, and it is impossible to distinguish, e.g., pH effects and carbonate ion effects. To overcome this problem, we have conducted experiments following both the classical approach, i.e., covarying pH and $\left[CO_3^{2-}\right]$, as well as keeping pH constant while varying $\left[CO_3^{2-}\right]$. The experimental setup used allows us hence to independently quantify effects of pH and $\left[CO_3^{2-}\right]$ on foraminiferal U/Ca. The carbonate chemistry perturbation experiments were conducted with specimens of the benthic foraminifer "*Ammonia molecular type T6*" [*Hayward et al.*, 2004] further referred to as *Ammonia* sp.

2. Material and Methods

2.1. Sample Collection and Culturing

[6] Surface sediments were collected from intertidal mudflats in the Wadden Sea (Dorum, Germany) at regular intervals between January and May 2011. Upon return to the laboratory, sediments were sieved over a 630 µm screen to remove macrofauna. Sieved sediment was transferred to small aquaria and covered with seawater collected at the same site. The aquaria were stored at 10°C and provided a set of stock cultures for the culturing experiments.

[7] From the stock material, specimens of *Ammonia* sp. were isolated by sieving sediment over a 230 µm screen. Living specimens were distinguished by having brightly colored yellow cytoplasm and pseudopodial activity. A number of specimens were transferred to well plates and placed at 25°C. Reproduction was stimulated by addition of food (living specimens of the green algae *Dunaliella salina*). Seawater was replaced and new food was added every 2–3 days. After 1 week, approximately 10% of the specimens had reproduced asexually, yielding 50–200 juveniles per specimen, consisting of a macrospheric proloculus (diameter approximately 40 µm). Juveniles were kept in well plates and fed for an additional 2–3 days, during which they added another approximately three chambers before being transferred to the controlled culture experiments.

2.2. Seawater Preparation

[8] Sterile-filtered North Sea water (0.2 µm pore size) was filled into an 80 L container and kept at 10°C in the dark. This batch was subsampled to determine pH, TA, and DIC. Culture media for the experiments were prepared from this batch by manipulating the carbonate chemistry in two different ways:

2.2.1. Experimental Set A: Acid/Base Manipulation

[9] Four sets of culture media were prepared by addition of acid (1 *M* HCl) or base (1 *M* NaOH). One culture medium consisted of not-manipulated seawater (Table 1, treatment A2). Culture media of this experimental set are characterized by a range of pH values and $\left[CO_3^{2-}\right]$, while the total inorganic carbon concentration was kept constant.

2.2.2. Experimental Set B: pH-Stable Manipulation

[10] In this set of experiments, seawater was manipulated by adjusting the $\left[CO_3^{2-}\right]$, while keeping pH stable. The four treatments were chosen, such that the accompanying pCO_2 values matched those of the acid/base manipulation (Table 1).

[11] To manipulate the carbonate ion concentration, calculated volumes of a bicarbonate stock solution were added to seawater. In one treatment (B1), the target carbonate ion concentration was lower than that of seawater; consequently DIC was reduced prior to addition of bicarbonate. This was achieved by acidification of the seawater with HCl (1510 µL 1 *M* HCl/L sw) followed by bubbling with CO_2 free air, to strip out DIC in the form of CO_2. Carbonate ion concentration was then determined first and

Table 1. Carbonate System Parameters, U/Ca, and D_U (Calculated Partition Coefficient)[a]

	Treatments							
	A1	A2	A3	A4	B1	B2	B3	B4
pCO_2 (µatm) "nominal"	180	380	950	1400	180	380	950	1400
pCO_2 (µatm)	217	479	850	1301	63	396	829	1252
CO_3^{2-} (µmol/kg-sw)	401	224	136	88	21	152	405	563
HCO_3^- (µmol/kg-sw)	1798	1999	2073	2063	223	1499	3536	5131
DIC (µmol/kg-sw)	2205	2236	2232	2187	246	1662	3965	5729
TA (µmol/kg-sw)	2747	2535	2400	2277	342	1884	4436	6343
pH total scale	8.32	8.02	7.79	7.60	7.95	7.98	8.03	8.01
Ω_{cc}	9.8	5.5	3.3	2.2	0.5	3.7	9.9	13.8
Salinity	32.8	32.8	32.8	32.8	32.7	32.7	32.8	32.6
U/Ca_{sw} (nmol/mol)	1344	1364	1365	1364	1366	1328	1354	1520
U/Ca_{cc} (nmol/mol)	32	43	106	117	797	187	25	27
$D_U \times 1000$	23	31	78	85	583	141	18	18

[a]U/Ca of the seawater media (sw) and calcite (cc) as well as calculated partition coefficient D_U for acid/base manipulation (A1–A4) and pH-stable manipulation (B1–B4) treatments. pH and DIC were measured and used as input parameters to calculate the carbonate system (together with salinity and temperature using the CO2SYS software [*Pierrot et al.*, 2006]). pCO_2 values supplied from the gas-mixing system are additionally listed (nominal). Average precision of DIC based on repeated measurements of an in-house standard was 10 µmol/kg-sw. Stability was checked over the course of the experiment by regular pH measurements and control of the pCO_2 provided by the gas-mixing system (precision approximately 10 µatm).

used to calculate the volume of the bicarbonate stock solution to be added.

[12] In each treatment for the pH-stable manipulation, pH was subsequently adjusted with HCl (1 *M*) and NaOH (1 *M*) to 8.0 (Table 1). All media were filled bubble-free into borosilicate flasks, sealed gas tight with Teflon-lined caps and kept at 3°C upon usage in the experiments.

2.3. Experimental Setup and Culturing

[13] Petri dishes containing manipulated seawater and juveniles were placed into one of four controlled pCO_2 boxes. These boxes were connected to a gas-mixing system, supplying water-saturated air with set pCO_2 (Table 1). Gas flow rates were kept constant and set to 60 L per hour, which is sufficient to allow complete replacement of the atmosphere inside the box six times each hour. Boxes were installed in a temperature-controlled room kept at 26°C and subjected to a day/light cycle (12 h/12 h). The pCO_2 values of the gas mixtures were checked regularly and did not vary more than 10 µatm. Borosilicate bottles containing the pre-mixed media were opened and stored in the appropriate controlled pCO_2 box for 2 days prior to being used in the experiment to allow for equilibration. Water was replaced and foraminifera were fed photosynthetically inactive (sterilized) algae (*D. salina*) every 2–3 days. The algae were centrifuged to minimize dilution of the culturing media through food addition (approximately 1% dilution per feeding event). Petri dishes were exchanged every 2 weeks, to minimize potential effects of bacteria growing on the bottom of the dishes. Foraminifera were kept in the dishes for 59–96 days, after which they were taken out and cleaned. Foraminiferal tests were placed in concentrated NaOCl for approximately 20 min to remove the cytoplasm. Specimens were subsequently rinsed three times in deionized water and dried at room temperature.

2.4. Sample Analysis

2.4.1. Seawater Composition: Elemental Concentrations and the Carbonate System

[14] The calcium concentration of the culture media was determined via ICP-OES (inductively coupled plasma optical emission spectrometry). Seawater uranium concentrations were calculated from salinity, using the re-evaluated U-salinity relationship in seawater from *Owens et al*. [2011].

[15] The DIC samples were filled without headspace into acid-washed 13 mL borosilicate flasks. Samples were measured within days and stored at 0°C until measurement. DIC was measured in duplicates photometrically [*Stoll et al*., 2001] with a TRAACS CS800 QuaAAtro autoanalyzer (Seal Analytica, Meqon, USA). Average precision was 10 µmol/kg-sw based on repeated measurements of an in-house standard calibrated against Batch No. 54 of A. Dicksons CRMS (Certified Reference Material Seawater, Marine Physical Laboratory, Scripps Institution of Oceanography). pH was measured potentiometrically using an NBS-calibrated glass electrode (Schott Instruments, Mainz, Germany) interfaced to a WTW pH meter. Conversion to the total scale was performed by means of a seawater buffer: Tris/Tris-HCl prepared according to the recipe described in *Dickson et al*. [2007]. pH values reported are always on the total scale. Salinity and temperature were measured with a conductivity meter (WTW Multi 340i), interfaced with a TetraCon 325 sensor.

[16] Not all parameters of the carbonate system can be measured directly. However, only two measurable parameters are required to calculate the full system. Depending on the choice of input parameters, differences in the calculated parameters can occur (for a more thorough discussion, see *Hoppe et al*. [2012]). The values reported in Table 1 were calculated from pH and DIC, measured directly upon manipulation and are supplemented by three additional types of input-parameter combinations in the Supporting Information[1] (See Table S1). The CO2SYS software adapted to Excel by *Pierrot et al*. [2006] was used to calculate the carbonate system with the equilibrium constants for K1 and K2 of *Mehrbach et al*. [1973] as reformulated by *Dickson and Millero* [1987]. All values, figures, tables, and regression equations in the text are based on the values given in Table 1.

2.4.2. Element Analysis: LA-ICP-MS

[17] Element concentrations of cleaned foraminiferal shells were determined using laser ablation inductively coupled plasma mass spectrometry (LA-ICP-MS) at Utrecht University [*Reichart et al*., 2003]. We used an Excimer laser (Lambda Physik) with GeoLas 200Q optics connected to a sector-field mass spectrometer (Element2, Thermo Scientific). Ablation beam diameter was set to 80 µm, and pulse repetition rate was 6 Hz with an

[1]All Supporting Information may be found in the online version of this article.

energy density at the sample surface of ~1 J/cm^2. Elemental concentrations were calculated from isotopic counts of ^{24}Mg, ^{26}Mg, ^{27}Al, ^{43}Ca, ^{44}Ca, ^{55}Mn, ^{88}Sr, and ^{238}U, assuming standard natural abundance ratios [*Jochum et al.*, 2011]. Analytical parameters of the MS were set such that it took 0.52 s for a complete cycle through all masses. ^{27}Al was monitored to identify potential surface contaminations in the ablation profiles. Between approximately every 10 measurements, a NIST SRM 610 silicate glass was ablated three times and an in-house matrix-matched calcite standard once [*Raitzsch et al.*, 2010]. The glass standard was ablated with an energy density of ~5 J/cm^2, the calcite standard was ablated with the same energy density as used for the foraminifera [*Dueñas-Bohórquez et al.*, 2009]. The ^{43}Ca isotope was used as internal standard, assuming 40 wt% calcium in calcite, whereas ^{44}Ca was used to check for consistency. We analyzed six specimens per treatment and carried out five to seven measurements per individual, summing up to 276 spot measurements in total. Five measurements were discarded, due to thin chamber walls and consequently short ablation profiles. Using calculated seawater U/Ca ratios, the partition coefficient for uranium in foraminiferal calcite (D_U) was calculated according to (cc = calcite, sw = seawater)

$$D_U = \frac{(U/\mathrm{Ca})_{\mathrm{calcite}}}{(U/\mathrm{Ca})_{\mathrm{seawater}}}.$$

3. Results

3.1. U/Ca$_{cc}$ and D_U

[18] The overall mean U/Ca$_{cc}$ ranges from 32 to 797 nmol/mol between the different treatments, resulting in a D_U of 23–584 × 10^{-3} (Table 1). Since highest U/Ca$_{cc}$ (797 nmol/mol) was measured on shells grown in media undersaturated with respect to calcium carbonate, SEM (scanning electron microscopy) micrographs of the shell surface were taken after LA-ICP-MS analysis. Surface features did not show signs of dissolution (Figure 1b), when compared to the shells grown in supersaturated waters (Figures 1a and 1c).

[19] Variability in U/Ca$_{cc}$, expressed as relative standard deviation (RSD), indicates a relatively homogenous U/Ca$_{cc}$ (~50% on average) over the range of pH/ $\left[CO_3^{2-}\right]$ (Figure 2) in the acid/base manipulation, whereas foraminiferal U/Ca$_{cc}$ in the pH-stable manipulation varies between ~25% and ~75%. Highest carbonate ion concentrations resulted in a high relative variability in U/Ca$_{cc}$. The average intra-individual RSD was on average slightly lower (44%) than the average inter-individual RSD (51%). The associated uncertainty when measuring U/Ca$_{cc}$ on a number of specimens can be calculated from the RSD: the estimated standard error when measuring five individuals would be 23% and when measuring 10 individuals 16%. The detection limit for U in foraminiferal calcite was calculated as described in *Longerich et al.* [1996], which was on the order of 1 × 10^{-5} ppm, approximately four orders of magnitude lower than measured uranium in cultured foraminifers.

3.2. Correlation Between D_U and the Carbonate System

[20] The correlation of D_U with the carbonate system parameters (pH, $\left[CO_3^{2-}\right]$, etc.) was analyzed by means of regression analysis (Table 2). All regressions are highly significant ($p < 0.001$), despite one, and from reported R^2 values, a correlation with all parameters but pH and pCO_2 seems possible and is discussed further below (section 4.1). An exponential correlation results in higher R^2 values, seeming thus more likely. Tukey post hoc

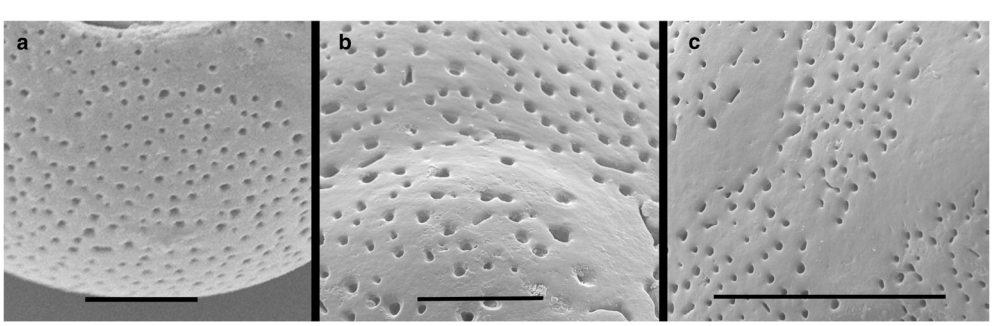

Figure 1. The SEM images of cultured *Ammonia* sp. shell surfaces. ((a) Specimen from treatment A2 ("control group"—modern day carbonate system parameters, Ω_{Ca} = 5.5), scale bar represents 20 μm. (b) Specimen from treatment B1 with the lowest Ω_{Ca} (0.5), scale bar = 20 μm. (c) Specimen from treatment B4 with the highest Ω_{Ca} (13.8), scale bar = 50 μm.

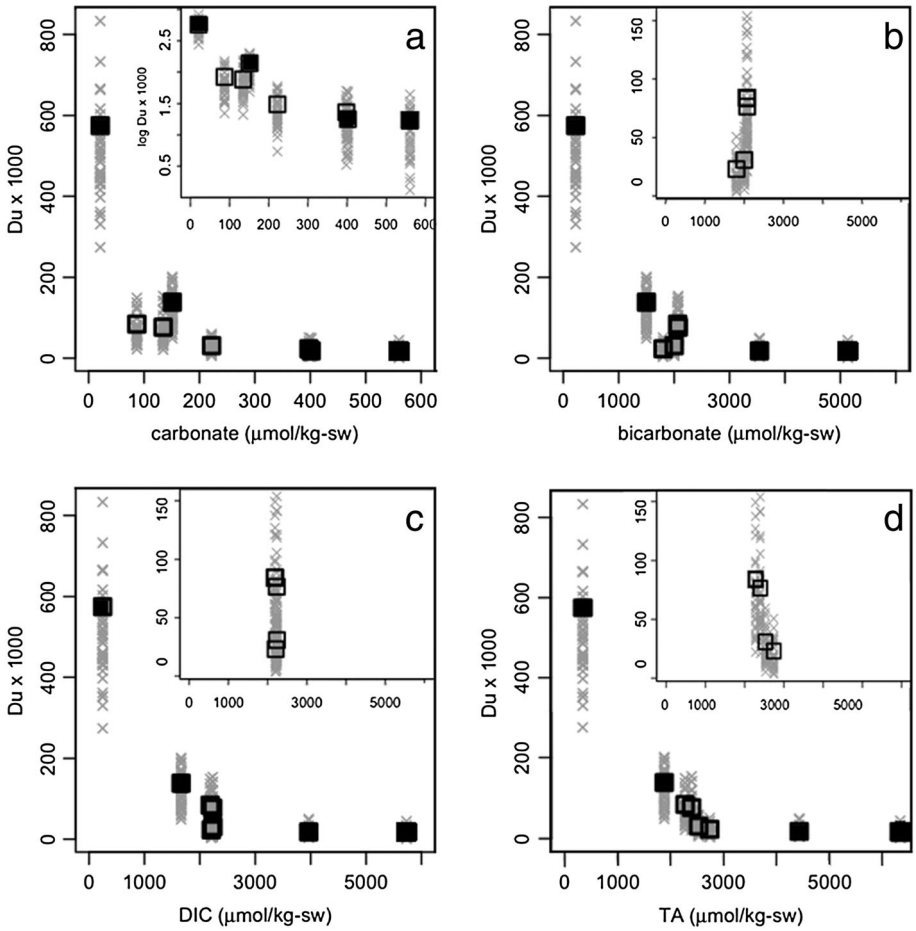

Figure 2. The D_U (Log D_U) versus (a) carbonate, (b) bicarbonate, (c) DIC, and (d) TA in µmol/kg-sw. Grey crosses represent individual laser-ablation measurements, whereas squares indicate mean values. Open squares represent data from acid/base manipulation and closed squares from pH-stable manipulation. Figures 2a–2d contain data of all treatments combined. Inset in Figure 2a depicts Log D_U versus carbonate (µmol/kg-sw). Insets in Figures 2b–2d represent data from the acid/base manipulation only; labeling for *x* and *y* axes is the same as in Figures 2b–2d and has been omitted. Please note that depiction of treatments A1 and B3 overlaps in Figure 2a (nearly identical D_U values at a carbonate ion concentration of approximately 400 µmol/kg-sw).

tests (see Supporting Information for more details on statistical treatment) were performed to determine which treatments (based on D_U) were statistically different from each other, and the results also support an exponential correlation (here explained with $[CO_3^{2-}]$ as an example, see Figure S1): On the higher end of the carbonate ion concentration (>200 µmol/kg-sw), D_U values are statistically indifferent from each other (e.g., A1 and B3). For carbonate ion concentration <100 µmol/kg-sw, all D_U are statistically different. This pattern fits a negative exponential correlation between D_U and carbonate ion concentration due to the mathematical properties of the exponential function. However, it has to be stressed that changes in carbonate ion concentration values at the lower end of the carbonate ion concentration (especially <100 µmol/kg-sw) range yield high differences in D_U, whereas those changes at the higher end of the concentration range yield only small or no appreciable changes in D_U.

4. Discussion

4.1. Correlation Between D_U and the Carbonate System

[21] We used two different methods to manipulate the seawater carbonate chemistry: an acid/base manipulation (treatments A1–A4, see Table 1) and a pH-stable manipulation (treatments B1–B4, see Table 1). Since the carbonate system parameters covary differently in the two experimental approaches, it is possible, by exclusion, to reject certain parameters of the carbonate system as causes for the observed changes in D_U (Table 1). In the acid/base

Table 2. The D_U Relationships With Carbonate System Parameters[a]

	R^2	p
$D_U = 239(\pm27)–0.55(\pm0.09)\ [CO_3^{2-}]$	0.35	<0.001
Log $D_U = 2.30(\pm0.07)–0.0027(\pm0.0002)\ [CO_3^{2-}]$	0.65	<0.001
$D_U = 286(\pm29)–0.06(\pm0.01)$ [TA]	0.42	<0.001
Log $D_U = 2.43(\pm0.08)–2.78 \times 10^{-4}(\pm0.25 \times 10^{-4})$ [TA]	0.63	<0.001
$D_U = 240(\pm27)–22.47(\pm3.68)$ [Ω]	0.35	<0.001
Log $D_U = 2.30(\pm0.07)–0.11(\pm0.01)$ [Ω]	0.65	<0.001
$D_U = 282(\pm29)–0.08(\pm0.01)\ [HCO_3^-]$	0.41	<0.001
Log $D_U = 2.39(\pm0.09)–3.26 \times 10^{-4}(\pm0.33 \times 10^{-4})\ [HCO_3^-]$	0.58	<0.001
$D_U = 283(\pm29)–0.07(\pm0.01)$ [DIC]	0.42	<0.001
Log $D_U = 2.41(\pm0.09)–2.97 \times 10^{-4}(\pm0.29 \times 10^{-4})$ [DIC]	0.60	<0.001
$D_U = 782(\pm814)–84.74(\pm102.30)$ [pH]	0.01	0.06
Log $D_U = 9.91(\pm2.76)–1.04(\pm0.35)$ [pH]	0.11	<0.001
$D_U = 244(\pm30)–0.19(\pm0.04)$ [pCO_2]	0.19	<0.001
Log $D_U = 2.09(\pm0.11)–6.07 \times 10^{-4}(\pm1.33 \times 10^{-4})$ [pCO_2]	0.14	<0.001

[a]Regression and statistics are based on individual measurements ($n = 271$ in total for all treatments). 95% confidence intervals are reported for intercepts and slopes of regressions. Units: $D_U = 1000 \times D_U$ and Log D_U = Log $1000 \times D_U$).

manipulation D_U displays a positive correlation with pCO_2, whereas the correlation of D_U and pCO_2 is negative in the pH-stable manipulation. Therefore, pCO_2 cannot be the parameter of the carbonate system causing a change in D_U. The change in D_U under constant pH (pH-stable manipulation) was almost a factor of 10 larger than in the acid/base manipulation, where pH covaried. Consequently, pH can be excluded as a controlling factor and the negative correlation of D_U with pH in the acid/base manipulation must be regarded as inherent to the carbonate system and not causal.

[22] In the pH-stable manipulation experiments, TA, DIC, $[HCO_3^-]$, $[CO_3^{2-}]$, and Ω correlate negatively with D_U over a wide range of values (Table 1 and Figure 2 closed squares; note that the correlation of D_U with Ω has not been plotted, since $[Ca^{2+}]$ was kept constant and consequently the distribution of Ω is essentially that of $[CO_3^{2-}]$; Figure 2a). By contrast, the ranges covered in the acid/base manipulation are, with the exception of $[CO_3^{2-}]$ and Ω, much smaller (Table 1). In the case of DIC (acid/base manipulation), most D_U are similar. Nevertheless, when D_U is plotted versus DIC, a conspicuous clustering of values can be seen, namely the D_U of treatments A3 and A4 are similar, and so are the D_U of treatments A1 and A2 (small inset in Figure 2c). The same clustering is obvious when D_U is plotted versus $[HCO_3^-]$ and TA (insets in Figures 2b and 2d). Combining values of the acid/base and the pH-stable manipulation in one plot (Figures 2b–2d) might, especially in the case of TA (Figure 2d), suggest that TA causes the change in D_U and that the curious clustering of treatments A3 and A4, and A1 and A2, respectively, simply reflects the transition of the curve from a steep to a shallow slope. If DIC or $[HCO_3^-]$ was the controlling factor, D_U values should be more or less identical in the pH-stable manipulation, given the small range in DIC and $[HCO_3^-]$. Since there is no reason why, given identical DIC/$[HCO_3^-]$, there should be such a distinct cluster pattern, and DIC and $[HCO_3^-]$ cannot be the parameter affecting D_U. The cluster pattern, however, is absent when plotting D_U versus $[CO_3^{2-}]$ (Figure 2a). Hence, based on the correlations only, $[CO_3^{2-}]$ or Ω are likely candidates to be instrumental in changing D_U, but leave open the possibility that TA might still be involved. It has to be noted, that Ca^{2+} was kept constant in all treatments and foraminifera do not respond to Ω as such, but to the concentrations of Ca^{2+} and CO_3^{2-} (which also holds true for TA) [*Dueñas-Bohórquez et al.*, 2011; *Raitzsch et al.*, 2010]. Consequently, the correlation between D_U and Ω is only caused by the concentration change in carbonate ions, leaving carbonate ions as the only candidate affecting foraminiferal U/Ca. Furthermore, we cannot exclude the possibility of parameters, such as TA and/or pH, exerting a modulating influence on the obtained correlations. While the modulating influence cannot be unambiguously identified using the data set presented here, we will point out that the correlation can be explained by a sole influence of carbonate ion concentration on D_U. Hence, a modulating influence of other parameters, although possible, is not needed in order to interpret the changes in D_U.

[23] The effect of $[CO_3^{2-}]$ on foraminiferal U incorporation could be explained in terms of uranium speciation in seawater. Uranium easily complexes with carbonate ions, and speciation thus strongly depends on $[CO_3^{2-}]$ of the seawater (Figure 3). With increasing $[CO_3^{2-}]$, the percentage of the

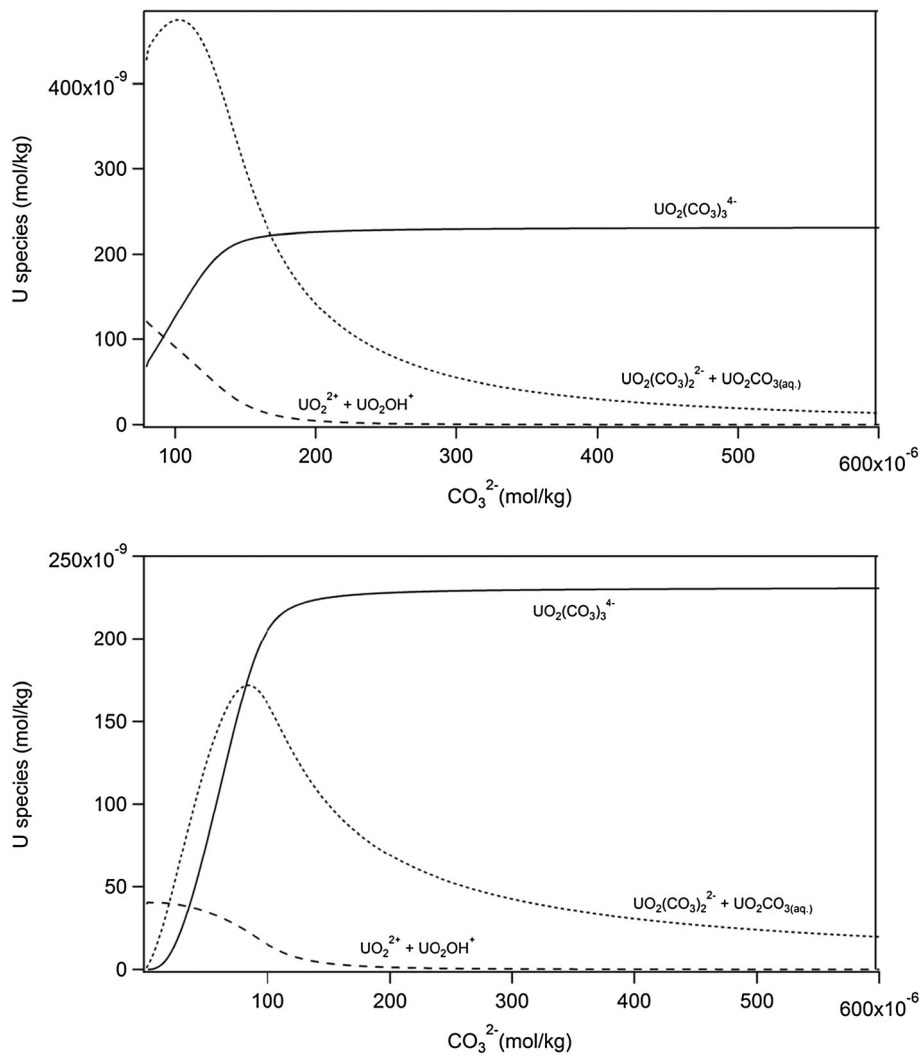

Figure 3. Uranium speciation as a function of carbonate ion concentration. Conditions of acid/base manipulation are seen in the top image and of pH-stable manipulation in the bottom image. Chemical speciation calculations were performed with the software Visual Minteq ver. 3.0 [*Gustafsson*, 2010]. The original thermodynamic database supplied with the software was used without alteration. The main components added to simulate a seawater water matrix were Ca^{2+} (10 m*M*), Mg^{2+} (60 m*M*), Na^{+} (0.7 *M*), and Cl^{-} (0.7 *M*). The speciation of the carbonate and uranium system for the two experimental manipulations (acid/base manipulation and pH-stable manipulation) was calculated as follows: the acid/base manipulation was represented by an open system where the pH was allowed to vary (calculated from the mass balance) and the pH-stable manipulation was represented by a closed system with a pH fixed at 8.2. H^{+} concentration and pCO_2 have been adjusted to fit the $\left[CO_3^{2-}\right]$ range of interest. All calculations were performed using a temperature of 25°C.

sum of the different carbonate complexes [$UO_2(CO_3)$(aq)], $\left[UO_2(CO_3)_3^{4-}\right]$, and $\left[UO_2(CO_3)_2^{2-}\right]$ increases, whereas the percentage of the sum of the free forms $\left[UO_2^{2+}\right]$ and [UO_2OH^{+}] decreases. This change in speciation is not linear and particularly prominent below ~200 µmol/kg-sw $\left[CO_3^{2-}\right]$ (Figure 3). Interestingly, the correlation of foraminiferal D_U with $\left[CO_3^{2-}\right]$ is also not linear, but exponential (see Figure 2a), with the largest change in D_U µmol/kg-sw $\left[CO_3^{2-}\right]$ at the lower range of $\left[CO_3^{2-}\right]$ used here, i.e., below ~200 µmol/kg-sw (Table 1 and Figure 2). This matches the increase in $\left[UO_2^{2+}\right]$ and [UO_2OH^{+}] at low $\left[CO_3^{2-}\right]$. We hypothesize that the free forms ($\left[UO_2^{2+}\right]$ and [UO_2OH^{+}]) are more readily taken up by *Ammonia* sp. than the carbonate complexes. This speculation would explain the observed dependency of D_U on $\left[CO_3^{2-}\right]$. In support of this hypothesis, it was reported that the bioavailability of U (i.e., its ability to bind to or traverse the cell surface) in green algae

increases with decreasing $\left[CO_3^{2-}\right]$ [*Fortin et al.*, 2004; *Markich*, 2002]. The latter authors attribute this effect to the fact that primarily the free forms of U (especially $\left[UO_2^{2+}\right]$) are taken up by the cells. In analogy, we speculate that the free forms of U can cross the cell membrane of *Ammonia* sp. more easily than the carbonate complexes can. This would imply that U is taken up via transmembrane transport during chamber formation, which therewith would be a major pathway of ion transport for chamber formation in *Ammonia* sp. The latter assumption was also put forth in the context of proton transport [*Glas et al.*, 2012]. We are aware that ion transport in foraminifera is usually assumed to be endocytosis mediated [*Erez*, 2003], but the latter hypothesis is based on experiments with a different species, and there might be species-specific differences in transport mechanism. We will point out that our explanation of the change in D_U with seawater $\left[CO_3^{2-}\right]$ is consistent with a constancy of U fractionation during calcite precipitation. This is advantageous, because pH homeostasis in the calcifying fluid most likely leads to a constant U speciation which would be decoupled from seawater U speciation.

4.2. Paleoceanographic Implications

[24] Previous studies [e.g., *Russell et al.*, 2004] reported a correlation between foraminiferal U/Ca and carbonate chemistry of seawater. While these studies attributed the effect to carbonate ion concentration/calcite saturation state, this inference remained conjectural, because in all available data sets, the parameters of the carbonate system covaried, rendering it impossible to tell, e.g., pH from carbonate ion effects. The reported U/Ca_{cc} values for benthic [*Raitzsch et al.*, 2011] and planktic foraminifera [*Russell et al.*, 2004] were 2–10 times lower than the ones determined by us for the same range of $\left[CO_3^{2-}\right]$ (80–110 µmol U/kg seawater). The difference in calcitic U/Ca_{cc} may be the result of species-specific fractionation against U during calcification and underscores the need for species-based calibrations when applying U/Ca_{cc} to reconstruct past $\left[CO_3^{2-}\right]$. However, it needs to be stressed that the species used here, *Ammonia* sp., is not commonly used in paleoceanographic studies, due to its shallow-water benthic habitat. Nevertheless, its abundance, easy accessibility, the relatively common asexual reproduction, and the tolerance of a broad range of environmental parameters make it a suitable candidate when determining basic foraminiferal responses. Applying the here-introduced experimental protocol of decoupling C-system parameters to more relevant species in terms of paleoceanography is a step that should be undertaken in the future to analyze the D_U-$\left[CO_3^{2-}\right]$ relationship further. While the slope of this relationship apparently is species specific, it is likely that the causal basis for this relationship is not. Our results therefore put the application of U/Ca_{cc} as a $\left[CO_3^{2-}\right]$ proxy on a firm footing.

[25] Even if not primarily of interest for paleoceanographic studies, a few properties of the correlation found here shall be given to facilitate comparability between different studies. The large range of $\left[CO_3^{2-}\right]$ applied in our culture study supports an exponential relation between carbonate ion concentration and calcitic U/Ca_{cc} as previously proposed by *Russell et al.* [2004]:

$$\mathrm{Log}\ U/\mathrm{Ca_{cc}} = 2.42(\pm 0.07) - 2.65 \times 10^{-3}\left(\pm 0.24 \times 10^{-3}\right)\left[CO_3^{2-}\right]$$

[26] Based on this calibration, we can infer that a decrease of 100 µmol/kg-sw in carbonate ion concentration from 300 to 200 µmol/kg-sw, as anticipated for a transition from full glacial to interglacial conditions, would be expected to result in an increase of 54% in foraminiferal U/Ca_{cc}. With our analytical approach, those changes can be quantified within the 95% confidence intervals. This sensitivity is approximately twice as high as that reported for two planktic species, *Orbulina universa* and *Globigerinoides sacculifer* by *Russell et al.* [2004].

5. Conclusion

[27] The partitioning coefficient for U in *Ammonia* sp., D_U, shows a negative correlation with TA, DIC, $\left[HCO_3^-\right]$, $\left[CO_3^{2-}\right]$, and Ω. By exclusion we argue that $\left[CO_3^{2-}\right]$ is the parameter controlling D_U. While *Ammonia* sp. might not be a species traditionally used in paleoceanographic reconstructions, the underlying processes of a carbonate chemistry-induced change in D_U are assumed to be the same for all foraminiferal species. Therefore, our data support the proposed use of foraminiferal U/Ca_{cc} as a $\left[CO_3^{2-}\right]$ proxy.

Acknowledgments

[28] We in particular wish to thank Caroline Otten for support with the culturing and Klaus-Uwe Richter for support with the experimental setup. Yvette Bublitz, Marc Bullwinkel, Antje Funcke, Jana Hölscher, Beate Müller, and Charlyn Völker are thanked for laboratory assistance. We thank Cathleen Zindler for unraveling the secrets of R. This research was funded by the Alfred Wegener Institute through Bioacid (Gerald Langer FKZ: 03F0608) and the European Community's Seventh Framework

Programme under grant agreement 265103 (Gerald Langer, Project MedSeA). This work contributes to EPOCA "European Project on Ocean Acidification" under grant agreement 211384. This work was funded in part by The European Research Council (ERC grant 2010-NEWLOG ADG-267931 HE). Nina Keul is the beneficiary of a doctoral grant from the AXA Research Fund.

References

Broecker, W. S., and T.-H. Peng (1982), Tracers in the Sea, 690 pp., Eldigeo Press, Lamont–Doherty Geological Observatory, Palisades, N.Y.

Dickson, A. G., and F. J. Millero (1987), A comparison of the equilibrium constants for the dissociation of carbonic acid in seawater media, *Deep-Sea Res.*, *34*(10), 1733–1743.

Dickson, A. G., C. L. Sabine, and J. R. Christian (Eds.) (2007), Guide to Best Practices for Ocean CO_2 Measurements, 191 pp., PICES Special Publication 3.

Dueñas-Bohórquez, A., M. Raitzsch, L. J. de Nooijer, and G.-J. Reichart (2011), Independent impacts of calcium and carbonate ion concentration on Mg and Sr incorporation in cultured benthic foraminifera, *Mar. Micropaleontol.*, *81* (3–4), 122–130.

Dueñas-Bohórquez, A., R. E. da Rocha, A. Kuroyanagi, L. J. de Nooijer, J. Bijma, and G.-J. Reichart (2009), Interindividual variability and ontogenetic effects on Mg and Sr incorporation in the planktonic foraminifer *Globigerinoides sacculifer*, *Geochim. Cosmochim. Acta*, *75*(2), 520–532.

Emiliani, C. (1955), Pleistocene temperatures, *J. Geol.*, *63*, 538–578.

Erez, J. (2003), The source of ions for biomineralization in foraminifera and their implications for paleoceanographic proxies, *Rev. Mineral. Geochem.*, *54*, 115–149.

Fortin, C., L. Dutels, and J. Garnier-Laplace (2004), Uranium complexation and uptake by a green alga in relation to chemical speciation: The importance of the free uranyl ion, *Environ. Toxicol. Chem.*, *23*(4), 974–981.

Glas, M. S., G. Langer, and N. Keul (2012), Calcification acidifies the microenvironment of a benthic foraminifer (*Ammonia* sp.), *J. Exp. Mar. Biol. Ecol.*, *424-425*(0), 53–58.

Gustafsson, J. P. (2010), Visual MINTEQ, Version 3.00. KTH, Dept. Of Land and Water Resources Engineering, Stockholm, Sweden.

Hayward, B. W., M. Holzmann, H. R. Grenfell, J. Pawlowski, and C. M. Triggs (2004), Morphological distinction of molecular types in *Ammonia*—Towards a taxonomic revision of the world's most commonly misidentified foraminifera, *Mar. Micropaleontol.*, *50*(3–4), 237–271.

Hemming, N. G., and G. N. Hanson (1992), Boron isotopic composition and concentration in modern marine carbonates, *Geochim. Cosmochim. Acta*, *56*(1), 537–543.

Hönisch, B., and N. G. Hemming (2005), Surface ocean pH response to variations in pCO_2 through two full glacial cycles, *Earth Planet. Sci. Lett.*, *236*, 305–314.

Hönisch, B., N. G. Hemming, D. Archer, M. Siddall, and J. F. McManus (2009), Atmospheric carbon dioxide concentration across the Mid-Pleistocene transition, *Science*, *324* (5934), 1551–1554.

Hönisch, B., et al. (2012), The geological record of ocean acidification, *Science*, *335*(6072), 1058–1063.

Hoppe, C. J. M., G. Langer, S. D. Rokitta, D. A. Wolf-Gladrow, and B. Rost (2012), Implications of observed inconsistencies in carbonate chemistry measurements for ocean acidification studies, *Biogeosciences 9*, pp. 2401–2405 doi:10.5194/bg-9-2401-2012.

IPCC (2007), Climate Change 2007: Synthesis Report. Contribution of Working Groups I, II and III to the Fourth Assessment Report of the Intergovernmental Panel on Climate Change., 104 pp., IPCC, Geneva, Switzerland.

Jochum, K. P., et al. (2011), Determination of reference values for NIST SRM 610–617 glasses following ISO Guidelines, *Geostand. Geoanal. Res.*, *35*(4), 397–429.

Longerich, H. P., S. E. Jackson, and D. Gunther (1996), Interlaboratory note. Laser ablation inductively coupled plasma mass spectrometric transient signal data acquisition and analyte concentration calculation, *J. Anal. Atom. Spectrom.*, *11* (9), 899–904.

Lüthi, D., et al. (2008), High-resolution carbon dioxide concentration record 650,000–800,000 years before present, *Nature*, *453*(7193), 379–382.

Markich, S. (2002), Uranium speciation and bioavailability in aquatic systems: An overview, *ScientificWorldJournal*, *2*, 707–729.

Mehrbach, C., C. H. Culberson, J. E. Hawley, and R. M. Pytkowicz (1973), Measurement of the apparent dissociation constants of carbonic acid in seawater at atmospheric pressure, *Limnol. Oceanogr.*, *18*(6), 897–907.

Nürnberg, D., J. Bijma, and C. Hemleben (1996), Assessing the reliability of magnesium in foraminiferal calcite as a proxy for water mass temperatures, *Geochim. Cosmochim. Acta*, *60*(5), 803–814.

Owens, S. A., K. O. Buesseler, and K. W. W. Sims (2011), Re-evaluating the 238U-salinity relationship in seawater: Implications for the 238U-234Th disequilibrium method, *Mar. Chem.*, *127*(1–4), 31–39.

Pierrot, D., E. Lewis, and D. W. R. Wallace (2006), MS Excel Program Developed for CO_2 System Calculations., edited by O. R. N. L. ORNL/CDIAC-105. Carbon Dioxide Information Analysis Center, U.S. Department of Energy, Oak Ridge, Tennessee (2006).

Raitzsch, M., A. Dueñas-Bohórquez, G. J. Reichart, L. J. de Nooijer, and T. Bickert (2010), Incorporation of Mg and Sr in calcite of cultured benthic foraminifera: Impact of calcium concentration and associated calcite saturation state, *Biogeosciences*, *7*(3), 869–881.

Raitzsch, M., H. Kuhnert, E. C. Hathorne, J. Groeneveld, and T. Bickert (2011), U/Ca in benthic foraminifers: A proxy for the deep-sea carbonate saturation, *Geochem. Geophys. Geosyst.*, *12*(6), Q06019.

Reichart, G.-J., F. Jorissen, P. Anschutz, and P. R. D. Mason (2003), Single foraminiferal test chemistry records the marine environment, *Geology*, *31*(4), 355–358.

Russell, A. D., B. Hönisch, H. J. Spero, and D. W. Lea (2004), Effects of seawater carbonate ion concentration and temperature on shell U, Mg, and Sr in cultured planktonic foraminifera, *Geochim. Cosmochim. Acta*, *68*(21), 4347–4361.

Sanyal, A., N. G. Hemming, G. N. Hanson, and W. S. Broecker (1995), Evidence for a higher pH in the glacial ocean from boron isotopes in foraminifera, *Nature*, *373*(6511), 234–236.

Smith, A. D., and A. A. Roth (1979), Effect of carbon dioxide concentration on calcification in the red coralline alga *Bossiella orbigniana*, *Mar. Biol.*, *52*(3), 217–225.

Stoll, M. H. C., K. Bakker, G. H. Nobbe, and R. R. Haese (2001), Continuous-flow analysis of dissolved inorganic carbon content in seawater, *Anal. Chem.*, *73*(17), 4111–4116.

Yu, J., and H. Elderfield (2007), Benthic foraminiferal B/Ca ratios reflect deep water carbonate saturation state, *Earth Planet. Sci. Lett.*, *258*, 73–86.

Yu, J., G. L. Foster, H. Elderfield, W. S. Broecker, and E. Clark (2010), An evaluation of benthic foraminiferal B/Ca and $\delta^{11}B$ for deep ocean carbonate ion and pH reconstructions, *Earth Planet. Sci. Lett.*, *293*, 114–120.